A data-driven topology optimization approach to handle geometrical manufacturing constraints in the earlier steps of the design phase

Waad Almasri, Florence Danglade, Dimitri Bettebghor, Faouzi Adjed, Fakhreddine Ababsa

Available online at www.sciencedirect.com

ScienceDirect

Procedia CIRP 119 (2023) 377–383

www.elsevier.com/locate/procedia

33rd CIRP Design Conference

A data-driven topology optimization approach to handle geometrical manufacturing constraints in the earlier steps of the design phase

Waad ALMASRI[a,b], Florence DANGLADE[b], Dimitri BETTEBGHOR[a], Faouzi ADJED[a,c], Fakhreddine ABABSA[b]

[a]*Expleo France, 3 avenue des Prés, Montigny-le-Bretonneux 78180, France*

[b]*Laboratoire d'Ingénierie des Systèmes Physiques et Numériques (LISPEN), Arts et Métiers, 2 Rue Thomas Dumorey, Chalon-Sur-Saone 71100, France*

[c]*IRT SystemX, 2 Bd Thomas Gobert, 91120 Palaiseau, France*

* Corresponding author: Waad ALMASRI. Tel.:+33-1-3012-2500. *E-mail address:* waad.almasri@ensam.eu

Abstract

This paper improves on the performance of the Deep Learning Additive Manufacturing driven Topology Optimization (DL-AM-TO) approach that was proposed in [4]. DL-AM-TO is a data-driven generative method that integrates the mechanical and geometrical constraints concurrently at the same conceptual level and generates a 2D design accordingly. Furthermore, DL-AM-TO tailors the design's geometry to comply with manufacturing criteria, which facilitates the designer's interpretation phase and prevents him/her from getting stuck in a loop of drawing the CAD and testing its performance. The geometry needs less support structure and hence is printed faster. Consequently, DL-AM-TO accelerates the Design for AM process.

Keywords: Topology Optimization; Additive Manufacturing; Generative Design; Deep Learning.

1. Introduction

Along with their development, manufacturing systems replaced human involvement in the process one step at a time. Nowadays, humans are still present in the product lifecycle, from design to manufacturing. This process is known as the design for Additive Manufacturing (DfAM) process. Finding the solutions to blend this interaction is the only guarantee of a performant manufacturing system. Indeed, computer-aided technologies in the design, analysis, manufacture, and assembly phases optimized manufacturing systems regarding time and costs. Nevertheless, the phase with the highest impact on the overall product cost ($\geq 70\%$) is the design phase; it allows handling defects at a lower cost. From this, the concept of "first-time correct" has emerged. The goal is to find the most optimal and free-from-defects design at an early phase of the product's lifecycle [7]. Thus, much research has been put into exploring new approaches to accelerate the DfAM process.

We classify the state-of-the-art approaches proposed to accelerate the DfAM process into four major approaches.

The first one consisted of creating AM guidelines for design

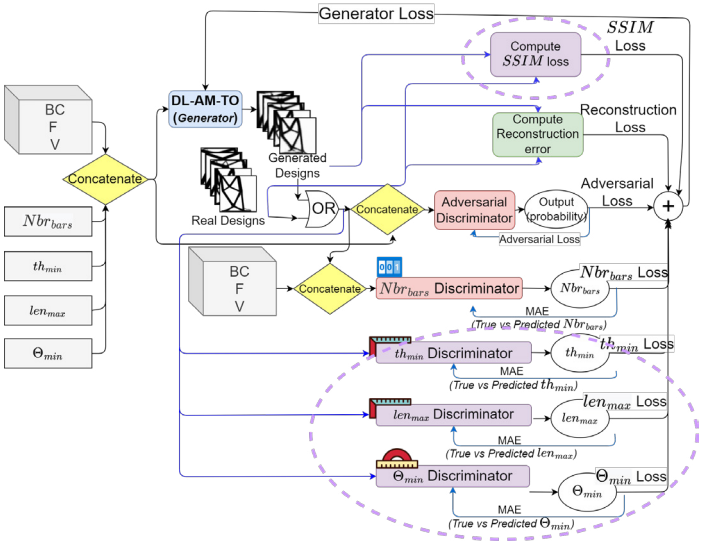

Fig. 1: DL-AM-TO's training procedure. The difference between this figure and the figure 3 in [4] consists of the addition of the structural similarity loss (L_{SSIM}) and the th_{min}, len_{max}, and Θ_{min} geometrical discriminators' architecture (in purple); in this work, they were converted from regression models to classification models.

10.1016/j.procir.2023.02.143

engineers to help them in the re-interpretation phase to draw AM-compliant designs. While this approach was a significant step into the adoption of design for AM, the designers still got stuck in the drawing phase due to the mechanical performance deterioration induced by updating the shape to comply with AM constraints [1, 8, 12].

Thus, for a reason mentioned previously, the second approach proposed integrating AM constraints into finite elements based TO (FE-TO) methods so that generated designs would be compliant with both mechanical and AM constraints simultaneously; the top common AM constraints are the minimum overhang [13, 6] or support structures [24], the thin features [10, 22]. Nevertheless, this approach faced several challenges. AM constraints are contradictory [25], informal [11], and geometrical), making formulating them analytically challenging, especially with FE-TO, the geometry is unknown beforehand. Moreover, FE-TO identifies the shape at early iterations, restraining it from changing to account for other constraints. Finally, FE-TO has a hard time converging [18] (i.e., finding the optimal design complying with all the constraints) with the increasing number of constraints, and when it converges, the computational power needed can be significantly expensive.

The third approach modeled a hybrid TO method; they replaced some FE blocks with Machine (ML) or Deep Learning (DL) techniques [16, 21, 9, 15]. Unfortunately, this approach focused on the design phase and not the whole DfAM process and inherited the convergence and computational flaws of FE.

The fourth approach replaced FE with ML/DL models [19, 14, 17]. This last approach accelerated TO and eliminated all FE-TO setbacks but did not integrate any AM constraints and did not impede getting stuck in a loop in later phases of the DfAM process.

We aim to accelerate the entire DfAM process and have the best quality/cost ratio. Indeed, the design phase is the least costly and the most impactful on the overall product cost [7]. Nevertheless, more than accelerating this phase is required, as we have seen with state-of-the-art approaches. Moreover, while AM-driven FE-TO methods aim to accelerate the whole DfAM process by preventing repetitive iterations, the analytical formulation of AM constraints, the methods' convergence, and their computational costs are still a hurdle. Conversely, the introduction of ML and DL only accelerated one phase. Thus, we propose to get the best of both worlds in this work; this new DL approach allows manufacturing constraints' integration within mechanical ones concurrently at the same level, and any constraints, even ones lacking a mathematical definition [23] like experts' rules and knowledge while benefiting from DL's speed and scalability advantages. Thus, DL-AM-TO, a TO approach based on DL that integrates AM and mechanical constraints concurrently at the same level, was proposed in [4]. DL-AM-TO is a generative model that takes as input the mechanical (Boundary conditions BC, loads F, volume fraction V) and geometrical (number of bars Nbr_{bars}, minimum thickness th_{min}, maximum length len_{max}, minimum overhang Θ_{min}) constraints and generates a 2D image-like design. The training designs and constraints come from the open-source dataset, Geometrical and Mechanical CAD (GMCAD) dataset [3], which was inspired by designs outputted by the top common industrial TO method, Solid Isotropic Material with penalization (SIMP) [5]. In [4], DL-AM-TO showed poor performance regarding the generated designs' quality. This behavior was identified to be tied to several criteria, the most impactful one being the geometrical discriminators' performance. The better the discriminator predicts the geometrical condition, the more informative the generator's loss function is; hence, DL-AM-TO is more reliable. We note that it is trained within GAN frameworks known for their unstable oscillating losses, which explains its sensitivity to the losses delivered by its discriminators. This phenomenon is observed with the th_{min} variable; integrating the latter into the model deteriorated its performance. The th_{min} discriminator should have been more precise. As a matter of fact, the image-like designs in GMCAD are CAD models converted to images with computer vision filtering techniques, which can easily alter the thicknesses of the design.

Consequently, to improve on the previous results, several actions are taken into consideration in this paper: (1) Improve the performance of the geometric discriminators, for their performance dramatically impacts the generator's performance. (2) Retrain DL-AM-TO with the new geometrical discriminators (Fig.1). (3) Propose several geometries for the same mechanical conditions using DL-AM-TO, draw these geometries, print them, and compare their manufacturability.

The major contribution of this article is validating the capability of DL-AM-TO to accelerate the whole DfAM, not simply the design phase. The article is organized as follows: section 2 details the geometric discriminators' improvement. DL-AM-TO's training is summarized in section 3. Sections 4 and 5 outline DL-AM-TO's performance. Section 6 presents DL-AM-TO's limitations. Finally, section 7 summarizes the methodology and its outcomes and presents future perspectives.

2. Improving the geometric discriminators' performance

The geometrical constraints are scalar values; thus, previously, we have chosen a regression-like architecture. Unfortunately, this architecture only convenes some constraints; th_{min} discriminator needed to be more precise. Hence, we decided to convert the regression problem into an ordinal regression one; it is a special case of classification problems. Instead of predicting the scalar value of a constraint, we will predict an interval in which it falls. The geometrical constraints that were concerned are len_{max}, th_{min}, and Θ_{min}.

The len_{max} constraint was divided into twenty-one classes (figure 3a). As described in [3], the len_{max} and th_{min} are measured with respect to the unit measure, with it being the width of the design space, which is equal to its height in our work.

The th_{min} constraint was divided into nine classes (figure 3b).

The Θ_{min} constraint was divided into fourteen classes (figure 3c). It is essential to highlight here that we exclude the rotational data augmentation for two reasons. First, the Θ_{min} is the only geometrical value affected by the rotation of the design space. Also, we realized that the distribution of Θ_{min} values after rotational data augmentation became not uniform and

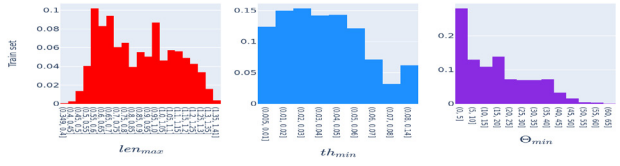

(a) Train set of len_{max} CORN discriminator.

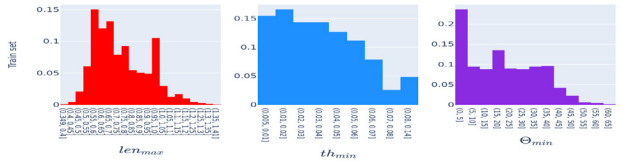

(b) Train set of th_{min} CORN discriminator.

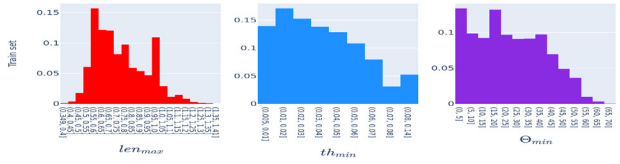

(c) Train set of Θ_{min} CORN discriminator.

Fig. 2: Distribution of the geometric intervals of len_{max}, th_{min}, & Θ_{min}, from left to right respectively, in the training sets of the len_{max}, th_{min}, & Θ_{min} CORN discriminators, from top to down respectively.

did not include all the value intervals for the designs present in GMCAD; thus, this data augmentation will affect the representativeness of some classes in the dataset and deteriorate the model's performance. Second, we train DL-AM-TO with no data augmentation; hence, the Θ_{min} discriminator is only needed to predict on non-rotated designs with Θ_{min} ranging from 0 to 70°.

To comply with the problem's formulation as a classification instead of a regression, the discriminators' architectures defined in [4] will only differ on the last fully connected layer; the output is a binary vector of K nodes with K being the number of classes of the variable described above; i.e., $K = 21$ for the len_{max} model, $K = 9$ for the th_{min} model, $K = 14$ for the Θ_{min} model.

The geometric discriminators are trained via the state-of-the-art Conditional Ordinal Regression for Neural networks (CORN) framework [20].

2.1. Training dataset

To further improve the geometric discriminator's accuracy, we have increased the number of training data samples per geometric variable to ensure that every class (i.e., every interval of values) is well represented. The distribution of the intervals of len_{max}, Θ_{min} and th_{min} values in the training set for every geometric discriminator is shown in figure 2.

2.2. Results

On the test set, the global accuracy score of the th_{min} is 93.7%, of $lenmax$ is 86.1%, and of Θ_{min} is 91.2%. However, when it comes to multi-class classification, the global macro accuracy score can be deceiving, and a better approach is to use the micro scores, i.e., scores per class. Thus, figure 3 plots the confusion matrices computed on the test set. We define an admissible misclassification as a point belonging to the class k classified into the class $k \pm 1$.

For the th_{min} discriminator, the highest percentage of admissible confusion is 16.77%, for the class $(0.07, 0.08]$; it is confused with the class $(0.08, 0.14]$, which is admissible. Moreover, the class $(0.07, 0.08]$ is the least represented class in the training set (figure 2b shows the distribution of the classes of th_{min}). As for the remaining classes, this percentage never exceeds the 8%. The highest percentage of inadmissible confusion is of 1.8%, for the class $(0.06, 0.07]$; with this class being confused by 0.53% with the class $(0.03, 0.04]$, 0.11% with the class $(0.03, 0.04]$, and 1.16% with the class $(0.08, 0.14]$.

For the len_{max} discriminator, the least accurate CORN discriminator, the highest percentage of admissible confusion is 82%, for the class $(0.349, 0.4]$; this class is the least represented class in the training dataset (0.05%, figure 2a), which makes it challenging for the model to predict the exact class. Nevertheless, the model confuses it with the exact following class $(0.4, 0.45]$, which is admissible. Similarly, the highest percentage of inadmissible confusion is 5.17% for the class $(0.45, 0.05]$.

For the Θ_{min} discriminator, the highest percentage of admissible confusion is 28.6%, for the class $(55°, 60°]$; it seems that angles belonging to $(55°, 60°]$ are highly confused with the class $(60°, 65°]$. As a matter of fact, this confusion is understandable, for these two classes are less represented than the others (figure 2c shows the distribution of the classes of Θ_{min}). The highest percentage of inadmissible confusion is 1.68%, for the class $(5°, 10°]$.

Finally, the global percentage of inadmissible predictions are 1.23% for len_{max} discriminator, 0.92% for the Θ_{min} discriminator, and 0.4% for the th_{min} discriminator. Thus, all three geometrical discriminators are precise enough to forward the training of DL-AM-TO.

3. Training DL-AM-TO with new discriminators

We recall DL-AM-TO's training procedure described in section 3 in [4]. First, the mechanical (the boundary conditions BC, the loads F, and the volume fraction V) and geometrical (the number of bars Nbr_{bars}, the minimum thickness th_{min}, the maximum length len_{max}, and the minimum overhang Θ_{min}) constraints are inputted to DL-AM-TO, which generates a 2D design accordingly. Second, this design is input to the th_{min}, len_{max}, and Θ_{min} discriminators, which predict its geometric constraints. Third, the design and the mechanical constraints are input to the Nbr_{bars} discriminator, which predicts its Nbr_{bars}. Fourth, the generated design and all input constraints are input to the traditional discriminator, which computes the

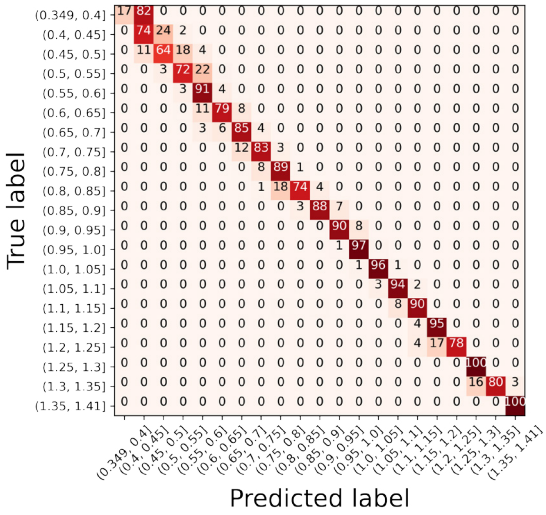

(a) len_{max} discriminator.

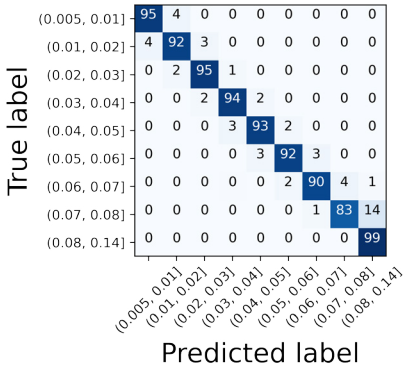

(b) th_{min} discriminator.

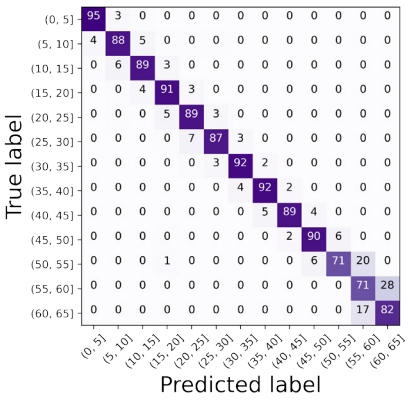

(c) Θ_{min} discriminator.

Fig. 3: The confusion matrices of the len_{max}, th_{min}, and Θ_{min} CORN discriminators computed on the test set.

probability of the design being real. Finally, the losses from the different discriminators are computed, summed, and fed to the generator to penalize it in case of non-conformity. The reconstruction and structural similarity losses are added for better training stability and guaranteed convergence.

With the new geometric discriminators, we retrain DL-AM-TO from [4]. Besides the geometric discriminators, we added the structural similarity loss (L_{SSIM}) to the training loss function.

$L_G = L_r + \lambda_{adversarial} L_{adv} + L_{Nbr_{bars}} + L_{th_{min}} + L_{len_{max}} + L_{\Theta_{min}} + L_{SSIM}$, with (1) the reconstruction loss $L_r = \frac{1}{N}\sum_{i=1}^{N}(x_i - \hat{x}_i)^2$ and $L_{SSIM} = 1 - \sum_{i=1}^{N}(\frac{(2\mu_{x_i}\mu_{\hat{x}_i}+k1)(2\sigma_{x_i\hat{x}_i}+k2)}{(\mu_{x_i}{}^2+\mu_{\hat{x}_i}{}^2+k1)(\sigma_{x_i}{}^2+\sigma_{\hat{x}_i}{}^2+k2)})$ s.t. x_i and $\hat{x}_i$ are the real and generated 2D design, N is the batch size, μ and σ the pixel sample mean and standard deviation, $k1$ and $k2$ are constants set to 0.01 and 0.03, respectively, (2) $\{L_c = \sum_{i=1}^{N}|c_i - \hat{c}_i|, c \in \{Nbr_{bars}, th_{min}, len_{max}, \Theta_{min}\}\}$ s.t. c and $\hat{c}$ are the input and predicted geometrical values respectively, and (3) the adversarial loss L_{adv} is the Binary Cross Entropy. $\lambda_{adversarial}$ was set to 0.01.

4. DL-AM-TO's overall performance

In the first version of DL-AM-TO [4], the authors reported an average Structural Similarity ($SSIM$) computed over the generated designs of 0.33, demonstrating a poor generation quality. In this work, the average $SSIM$ increased to 0.72, i.e., a 118% increase. This result validates our assumption that the geometrical discriminators' performance highly influences the generator's performance. Moreover, the global geometry of the design tells a lot about the placement of the loads and boundary conditions; thus, having a high $SSIM$ implies the conformity of the designs with these two mechanical constraints. To complete the mechanical performance, We also compute the energy of deformation (the compliance C in joules J) and volume fractions (the percentage of material in the design) of the DL-AM-TO designs and compare them to the metrics computed over SIMP designs. The metrics are the relative errors of volume fraction and compliance; the latter was computed using the FE method. 89.5% of the generated designs show a $V_{generated} \leq 1.1 \times V_{input}$. 44.4% of the generated designs show a compliance that is less or equal to 1.2 times the SIMP designs' compliance (i.e. $C_{generated} \leq 1.2 \times C_{ground-truth}$). It is important to note that the compliance is sensitive to intermediate density values. The compliance can be deceiving when the design is modeled as an image with continuous values. For a fair mechanical performance comparison, it is better to draw the CAD designs of the SIMP and DL-AM-TO designs, then perform a FE analysis (section 5). Another solution would be to retrain DL-AM-TO with an additional compliance discriminator or run a few iterations of SIMP on the shape outputted by DL-AM-TO. Lastly, we examine the geometrical conformity of DL-AM-TO to the geometrical input values. The metric used is the difference $\Delta_X = X_{generated} - X_{input}$; $X \in len_{max}, th_{min}, \Theta_{min}$, and Nbr_{bars}. For the Nbr_{bars} constraint, the same metric used in [4] is used here to check the generated designs' conformity; If the absolute difference between the $|\Delta Nbr_{bars}| \leq 2$, the generated design is considered compliant with the Nbr_{bars} constraint, such that the Nbr_{bars} is predicted via the regression-based Nbr_{bars} discriminator. For the remaining geometrical constraints, a generated design is geometrically compliant if its geometrical value is, at most, distant by ± one class from the input value, such that the class value is predicted by the corresponding CORN geometrical discriminator.

96.3% of the generated designs are compliant with the len_{max}

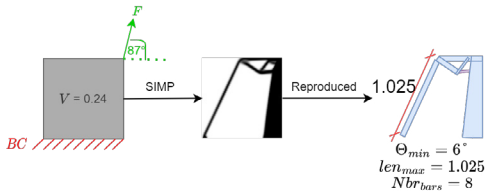

Fig. 4: Design generated by SIMP. This design is clamped on the bottom edge (*BC* in red), it is loaded on the top right corner (*F* in green), and the *V*

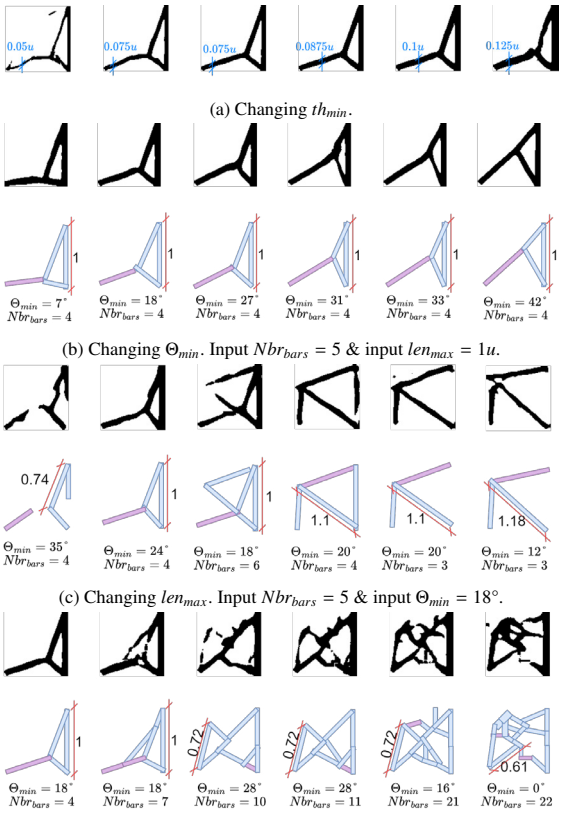

(a) Changing th_{min}.

(b) Changing Θ_{min}. Input $Nbr_{bars} = 5$ & input $len_{max} = 1u$.

(c) Changing len_{max}. Input $Nbr_{bars} = 5$ & input $\Theta_{min} = 18°$.

(d) Changing Nbr_{bars}. Input $len_{max} = 1u$ & input $\Theta_{min} = 18°$.

Fig. 5: Tailoring a geometrical constraint at a time.

constraint, 89.3% with the th_{min} constraint, 87.9% with the Θ_{min} constraint, and 88.7% with the Nbr_{bars} constraint.
On the computational performance, DL-AM-TO is thousands of times faster; it takes 0.03 seconds to generate a design, while SIMP needs 140 seconds to output the same design.
To recapitulate, DL-AM-TO generates designs with good quality and geometrically valid within a fraction of a second.

5. Tailoring a design's geometry with DL-AM-TO

For the sake of this article, we limited our experiments to one set of mechanical constraints (figure 4). This experiment tests DL-AM-TO's ability to tailor a design's geometry while always complying with mechanical constraints. Thus, we fix all input constraints except for one geometrical constraint. We scan a range of values for this constraint and generate the geometries accordingly. It is important to note that modifying the Nbr_{bars} and th_{min} constraints induce modifying the V, for increasing/decreasing these two constraints requires additional/less material as demonstrated in [2].

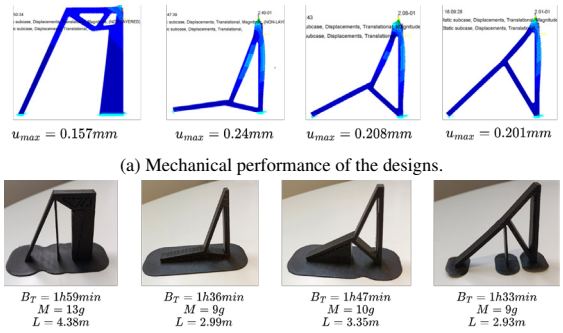

(a) Mechanical performance of the designs.

(b) Printed designs with support structures.

Fig. 6: Printing phase. The material used is the Polylactic acid (PLA). $\Theta_{min\,printer} = 60°$. u_{max} is the maximum displacement in *mm*. B_T is the build time. L and M are the PLA filament length and mass, respectively.

Figure 5 shows six geometries generated by DL-AM-TO after changing a geometrical constraint at a time.
Figure 5a illustrates the geometries outputted with increasing input th_{min}. As we can clearly see, DL-AM-TO generates designs thicker with the increasing th_{min} while respecting the other constraints; the shape is conserved, in other terms the *BC* and *F* are respected, the Nbr_{bars} vary in the range $Nbr_{barsinput} \pm 2$, which is admissible, the $len_{maxgenerated} = len_{maxinput} = 1u$, the $\Theta_{mingenerated} = \Theta_{mininput} = 18°$.
When Θ_{min} is modified, DL-AM-TO's generated geometries respect the len_{max} and Nbr_{bars} input constraints (figure 5b).
Figure 5c shows that the len_{max} of the generated geometries increases with the increasing input len_{max}. For the other constraints, the generated designs' Nbr_{bars} vary in the range $Nbr_{barsinput} \pm 2$, and their Θ_{min} in the range $\Theta_{mininput} \pm 6°$ (i.e., ± 1 class, section 2), except for the first geometry, which is admissible.
When the Nbr_{bars} is changed, we see that DL-AM-TO has difficulty conforming with the other geometrical constraints; 3 out of 6 geometries comply with the $\Theta_{mininput}$ and only 2 out of 6 comply with the $len_{maxinput}$. DL-AM-TO's non-conformity with len_{max} could be justified. DL-AM-TO adds bars to respect mechanical constraints, in other words, keeping the outer geometry intact, which makes that additional bars are internal transmission ones, which affects the len_{max} constraint that is reduced. On the other hand, the non-conformity with Θ_{min} is intriguing. This result should be further analyzed to understand the correlations between these two constraints.
To complete DL-AM-TO's evaluation, we chose the Θ_{min} experiment of figure 5b. We picked three designs generated by DL-AM-TO (the first, third, and last) and the one output by SIMP, drawn them using FreeCAD, tested their mechanical performance (measure by the maximum displacement u_{lmax}) using Patran/Nastran, and produced them using 3D printer Creality Ender 3; the support structures were added by the slicing software Cura. At every printing, we note the build time (B_T) and the length (L) mass (M) of the PLA material consumed to pro-

duce the part. We compare the mechanical and manufacturing metrics of the SIMP design versus the ones proposed by DL-AM-TO.

Figure 6b shows that DL-AM-TO designs are 30.7% cheaper in material (9g versus 13g for the SIMP design) and 10 to 22% faster to print while conserving the same mechanical performance as the one shown by SIMP; DL-AM-TO's designs show the same order of magnitude of u_{max} as the SIMP one (figure 6a).

To sum up, DL-AM-TO tailors design geometry to adapt it to manufacturing criteria. The test example described above demonstrates that DL-AM-TO proposes different geometries printable up to 22% faster and 30% cheaper than the SIMP design without deteriorating the mechanical performance.

6. Discussion

It is imperative to note that this approach is not intended to replace robust FE-TO but to help compensate for its difficulties in integrating various complex constraints. Indeed, a better approach would be a hybrid approach with the first draft generated by DL-AM-TO and the final optimized by an FE-TO method.

DL-AM-TO's capability to tailor a design's geometry was demonstrated in section 5. However, as we have noticed, when the Nbr_{bars} constraint is modified, DL-AM-TO has difficulty complying with the other constraints. This result can be explained in different ways: this constraint is correlated with the other geometrical constraints and seems to dominate over them. Hence, it would be interesting to push the analysis further and train several DL-AM-TO models with one geometrical constraint at a time to understand the influence of every constraint on the others when controlled alone to understand their correlations when controlled altogether eventually.

7. Conclusion

This paper improves on the setbacks reported in [4]. It proposes and validates a Deep Learning-based Additive Manufacturing driven Topology Optimization approach called DL-AM-TO. DL-AM-TO integrates the mechanical and geometrical constraints at the same level and generates 2D designs. More interestingly, it tailors the design's geometry easily to propose several geometries AM compliant corresponding to the engineer's input while keeping a similar mechanical performance as the one proposed by SIMP.

In the future, a pushed analysis of the correlations between the geometrical manufacturing-related constraints and further tests will be conducted and published to validate DL-AM-TO's performance and quantify its acceleration on the overall DfAM process. Additionally, DL-AM-TO could be enhanced to generate 3D designs. Finally, DL-AM-TO could be industrialized as a light and fast generative module in industrial design software.

References

[1] Adam, G.A., Zimmer, D.. Design for additive manufacturing—element transitions and aggregated structures. CIRP Journal of Manufacturing Science and Technology 7, 2014, 20–28.

[2] Almasri, W., Bettebghor, D., Ababsa, F., Danglade, F., Adjed, F.. Deep learning architecture for topological optimized mechanical design generation with complex shape criterion, in: International Conference on Industrial, Engineering and Other Applications of Applied Intelligent Systems, Springer, 2021. pp. 222–234.

[3] Almasri, W., Bettebghor, D., Adjed, F., Ababsa, F., Danglade, F.. Gmcad: an original synthetic dataset of 2d designs along their geometrical and mechanical conditions. Procedia Computer Science 200, 2022a, 337–347.

[4] Almasri, W., Danglade, F., Bettebghor, D., Adjed, F., Ababsa, F.. Deep learning for additive manufacturing-driven topology optimization. Procedia CIRP 109, 2022b, 49–54.

[5] Bendsøe, M.P.. Optimal shape design as a material distribution problem. Structural optimization 1, 1989, 193–202.

[6] Bi, M., Tran, P., Xie, Y.M.. Topology optimization of 3d continuum structures under geometric self-supporting constraint. Additive Manufacturing 36, 2020, 101422.

[7] Bi, Z., Wang, X.. Computer aided design and manufacturing. John Wiley & Sons, 2020.

[8] Booth, J.W., Alperovich, J., Reid, T.N., Ramani, K.. The design for additive manufacturing worksheet, in: International Design Engineering Technical Conferences and Computers and Information in Engineering Conference, American Society of Mechanical Engineers, 2016. p. V007T06A041.

[9] Chandrasekhar, A., Suresh, K.. Tounn: Topology optimization using neural networks. Structural and Multidisciplinary Optimization , 2020, 1–15.

[10] Fernández, E., Yang, K.k., Koppen, S., Alarcón, P., Bauduin, S., Duysinx, P.. Imposing minimum and maximum member size, minimum cavity size, and minimum separation distance between solid members in topology optimization. Computer Methods in Applied Mechanics and Engineering 368, 2020, 113157.

[11] Gao, W., Zhang, Y., Ramanujan, D., Ramani, K., Chen, Y., Williams, C.B., Wang, C.C., Shin, Y.C., Zhang, S., Zavattieri, P.D.. The status, challenges, and future of additive manufacturing in engineering. Computer-Aided Design 69, 2015, 65–89.

[12] Gaynor, A.T., Guest, J.K.. Topology optimization considering overhang constraints: Eliminating sacrificial support material in additive manufacturing through design. Structural and Multidisciplinary Optimization 54, 2016, 1157–1172.

[13] Han, Y.S., Xu, B., Zhao, L., Xie, Y.M.. Topology optimization of continuum structures under hybrid additive-subtractive manufacturing constraints. Structural and Multidisciplinary Optimization 60, 2019, 2571–2595.

[14] Malviya, M.. A systematic study of deep generative models for rapid topology optimization , 2020.

[15] Nie, Z., Lin, T., Jiang, H., Kara, L.B.. Topologygan: Topology optimization using generative adversarial networks based on physical fields over the initial domain. arXiv preprint arXiv:2003.04685 , 2020.

[16] Oh, S., Jung, Y., Lee, I., Kang, N.. Design automation by integrating generative adversarial networks and topology optimization, in: ASME 2018 International Design Engineering Technical Conferences and Computers and Information in Engineering Conference, American Society of Mechanical Engineers Digital Collection, 2018.

[17] Rade, J., Balu, A., Herron, E., Pathak, J., Ranade, R., Sarkar, S., Krishnamurthy, A.. Physics-consistent deep learning for structural topology optimization. arXiv preprint arXiv:2012.05359 , 2020.

[18] Ranjan, R., Samant, R., Anand, S.. Integration of design for manufacturing methods with topology optimization in additive manufacturing. Journal of Manufacturing Science and Engineering 139, 2017.

[19] Sharpe, C., Seepersad, C.C.. Topology design with conditional generative adversarial networks, in: International Design Engineering Technical Conferences and Computers and Information in Engineering Conference, American Society of Mechanical Engineers, 2019. p. V02AT03A062.

[20] Shi, X., Cao, W., Raschka, S.. Deep neural networks for rank-consistent

ordinal regression based on conditional probabilities. arXiv preprint arXiv:2111.08851 , 2021.

[21] Sosnovik, I., Oseledets, I.. Neural networks for topology optimization. Russian Journal of Numerical Analysis and Mathematical Modelling 34, 2019, 215–223.

[22] Yamada, T., Noguchi, Y.. Topology optimization with a closed cavity exclusion constraint for additive manufacturing based on the fictitious physical model approach. Additive Manufacturing 52, 2022, 102630.

[23] Zhang, K., Cheng, G.. Three-dimensional high resolution topology optimization considering additive manufacturing constraints. Additive Manufacturing 35, 2020, 101224.

[24] Zhang, K., Cheng, G., Xu, L.. Topology optimization considering overhang constraint in additive manufacturing. Computers & Structures 212, 2019, 86–100.

[25] Zhou, M., Liu, Y., Lin, Z.. Topology optimization of thermal conductive support structures for laser additive manufacturing. Computer Methods in Applied Mechanics and Engineering 353, 2019, 24–43.